BIOCIDAL CAPABILITY OF NANOCOMPOSITES BASED ON POLYPROPYLENE AND TITANIA

Marta Fernández-García[a], Cristina Serrano[a], Manuel Sánchez-Chaves[a], María L. Cerrada[a], Anna Kubacka[b], Manuel Ferrer[b], Marcos Fernández-García[b]

[a]Instituto de Ciencia y Tecnología de Polímeros, CSIC,C/Juan de la Cierva 3,28006-Madrid, Spain
[b]Instituto de Catálisis y Petroleoquímica, CSIC, C/Marie Curie 2, 28049-Madrid, Spain

ABSTRACT

TiO_2-isotactic polypropylene (iPP) nanocomposites with different inorganic component content were prepared via a straightforward and cost-effective melting process using laboratory-made nanometric anatase-TiO_2 and an industrial polymer. The structural characteristics of the resulting nanocomposite thin films as a function of the inorganic component content were examined using wide and small angle X-ray scattering (WAXS/SAXS) and vibrational Raman spectroscopy. Electron scanning and transmission microscopy (SEM/TEM) studies were also performed to provide evidence of the nanometric dispersion of the oxide within the polymer matrix. The presence of average aggregates of ca. 80 nm TiO_2 incorporation into the iPP renders self-sterilized nanocomposites films upon light excitation, their activity being tested against Gram negative (*P. aeruginosa*) and positive (*E. faecalis*) bacteria. TiO_2 displays maximum activity for a sample containing a 2 wt. % of anatase-TiO_2 irrespective of the microorganism nature. The antimicrobial activity of the nanocomposite films is significantly enhanced with respect to that exhibited by the oxide alone. Previous to that, the optimization of the interfacial agent content in biocidal titania-isotactic polypropylene nanocomposites was performed by evaluation of their structural, thermal, optical and biocidal properties. A compatibilizer content of 80 wt% with the respect to the titania amount was chosen as optimum composition.

Keywords: *Titania, Polypropylene, Nanocomposites, Biocide properties*

INTRODUCTION

The use of photocatalytic semiconductor oxides emerges as a successful technology to struggle against biological risks. TiO_2-anatase is by far the most widely used photocatalyst, being a wide band-gap (3.2 eV) semiconductor that under UV illumination generates energy-rich electron-hole pairs able to degrade cell components of microorganisms rendering innocuous products. Moreover, none weakness with respect to the microorganism nature (bacteria, virus, fungus, etc.) is nowadays known [1]. Consequently, its incorporation as a constituent in polymeric multicomponent materials could be a future alternative within goods packaging or biomedical fields and would open the current playground for photocatalysis application.

The important industrial success of isotactic polypropylene (iPP) and the wide range of its applications are basically due to the combination of outstanding physical properties (low density, high tensile strength, stiffness, and hardness, thermal and good environmental), ease of processability and recycling at a moderate cost [2]. Its non-polar macromolecular nature, however, makes the incorporation of functionalized oligomers as compatibilizers essential while hosting inorganic components. The discovery of single-site metallocene catalysts has determined great improvements and advantages in polymerization and copolymerization of olefins [3]. Taking into account their good transparency, their aesthetic and mechanical properties, metallocene-catalyzed polypropylene resins provide a replacement for glass in some critical uses, as packaging of species keeping their organoleptic qualities, and for others plastics, as polyvinyl chloride in medical devices. These novel fields as well as the current general uses of iPP, including automotive components, stationery and textiles (e.g. ropes, thermal underwear and carpets), among others, demand for improved polyolefin and, in particular, an important research area concerns the

possibility of adding bactericidal properties to such polymeric matrices [4]. Modification of these polymer-based systems to prevent growth or reduce adhesion of detrimental microorganisms appears thus a highly desired objective.

The goal of this work is to prepare, using a cost-effective melting processing, novel organic-inorganic nanocomposites based on titania and iPP with biocidal capabilities resulting from a nanometer anatase-TiO_2 component [5]. Previous to this, an optimization of the interfacial agent content to elaborate the nanocomposite is performed. As well known, the addition of an inorganic modifier can alter iPP structure and cristallinity, affecting in this way physical-chemical properties and demanding for a complete structural characterization of the whole system [6]. Through a multitechnique approach, the study aims to show that adequate incorporation of TiO_2 into a polymer-based nanocomposite film leads up to a powerful antimicrobial system, with a biocidal potential higher than that exhibited by the oxide alone. An efficient organo-inorganic contact changes the nature of the TiO_2 agent erasing the requirement of a close proximity with the pathogen, making the oxide in the nanocomposite a non-contact agent.

EXPERIMENTAL

The TiO_2 component was prepared using a microemulsion synthesis route by addition of titanium (IV) isopropide (Aldrich) to a inverse emulsion containing an aqueous phase dispersed in *n*-heptane (Panreac), using Triton X-100 (Aldrich) as a surfactant and 1-hexanol (Aldrich) as cosurfactant. The synthesis gives pure anatase with a primary particle size of 10 nm. A commercially available metallocene-catalyzed isotactic polypropylene, iPP (Basell Metalocene X50081: melt flow index of 60 g/10 min at 230 ^{o}C/2.16 kg, ASTM D1238), meeting FDA requirements (Federal Regulations, 21 CFR 177.1520) for food contact, was used as polymeric matrix in the preparation of iPP-TiO_2 nanocomposites with different TiO_2 nanoparticule contents: 0.5, 1, 2 and 5 wt%, labelled as Ti0.5, Ti1, Ti2 and Ti5, respectively. The Licomont® AR 504 fine grain from Clariant (a polypropylene wax partially modified with maleic anhydride, PPgMA) was added as a compatibilizer agent to improve the interfacial adhesion between the iPP and TiO_2. Use of PPgMA as an organic-inorganic compatibilizer is well established [7].

The crystal lattice characteristics of the nanocomposites were examined by wide angle X-ray scattering, WAXS, in the reflection mode at room temperature using a Rigaku Rotaflex RTP300 diffractometer connected to a computer having a Geiger counter and using a Ni-filtered Cu Kα radiation. The X-ray determinations of the degree of crystallinity were performed by subtraction of the corresponding amorphous component [8] comparing to the totally amorphous profile of an elastomeric PP sample. In addition, the transition associated with the melting process was investigated by real-time X-ray diffraction experiments with synchrotron radiation. The synchrotron studies were performed in the soft-condensed matter beamline A2 at Hasylab (Hamburg, Germany), working at a wavelength of 0.150 nm where two different detectors were used in the setup.

Raman and photoluminescence measurements were performed at room temperature with different laser lines of an Ar^{+}-Kr^{+} laser: 333 nm+365nm, and 514 nm. A home-made micro-Raman system was utilized. The EPR measurements were done with a Bruker ER200D spectrometer operating in the X-band and calibrated with a DPPH standard.

Scanning electron microscopy experiments for cross-section material analysis were carried out at room temperature in XL30 ESEM PHILIPS equipment working at 25 kV. Transmission electron microscopy experiments were carried out at room temperature in a 200 kV JEM-2000 FX JEOL microscope.

The microorganism used in this study included two clinical isolates: P. *aeruginosa* PAO clinical isolate PBCLOp11 from burn wound infections and E. *faecalis* clinical isolate brs30 from human biliary, both classified according to 165 rRNA (unpublished). To study the antimicrobial activity of the films, a suspension containing 10 µl of microbial cells (ca. 10^{9} cfu ml^{-1}) suspended in 1 ml broth solution was made as described elsewhere [9]. A minimum of three experimental runs was carried out to determine antimicrobial activity.

RESULTS AND DISCUSSION

Optimization of the interfacial agent content in biocidal titania-iPP nanocomposites at a given content of titania of 2 wt. % was performed by evaluating their structural, thermal, optical, and biocidal properties [10]. The influence of PPgMA content in the polymer/oxide crystalline characteristics, evaluated by WAXS and DSC, is rather insignificant for the different nanocomposites. However, the mobility of polymer amorphous regions is hindered leading to a slight improvement in thermal properties as compatibilizer content increases. These latest features seem to indicate a better adhesion to nanoparticle-polymer interfaces with contents of interfacial agent higher than 30 wt%, which appears corroborated by an enhancement of structural homogeneity on the interface according to SAXS and Raman. Photoluminescence measurements support the presence of oxide-born charge carriers in the materials with the two highest PPgMA compositions (50 and 80 wt. %) that efficiently interact and kill pernicious microorganisms and correlate well with the degree of nanoparticle-polymer interface adhesion. To conclude, it can be said that the ideal interfacial agent content for obtaining the most effective nanocomposite ranges from 50 to 80 wt%. This preparation method allows attaining cost-effective antimicrobial polymeric nanocomposites with an optimum interface adhesion between components, which may display significant advantages regarding either other solid-state methods such as ball milling which usually produces inhomogeneities in the system (e.g., molecular weight segregation) or inherently expensive preparation methods using chemical modification of organic and/or inorganic components and/or liquid-phase (solution processing) or in situ polymerization.

After this previous analysis, a compatibilizer content of 80 wt% with respect to the titania amount is chosen as optimum composition. Then, nanocomposites with different TiO_2 composition were prepared and the structural characteristics of the resulting thin films were examined using wide and small angle X-ray scattering (WAXS/SAXS) and vibrational Raman spectroscopy. Electron scanning and transmission microscopy (SEM/TEM) studies were also carried out to provide evidence of the nanometric dispersion of the oxide within the polymer matrix.

The iPP matrix and all the iPP-TiO_2 nanoparticulated composite thin films are semicrystalline as their WAXS profiles (reflection mode) at room temperature, depicted in Fig. 1, indicate.

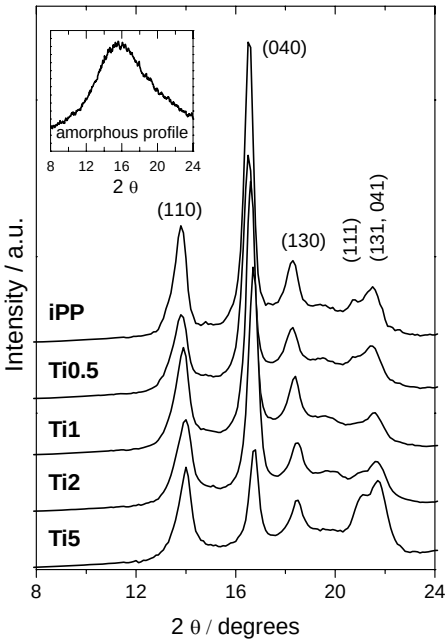

Figure 1. WAXS profiles at room temperature of different Tix nanocomposites and reference iPP. Inner plot: WAXS profile of amorphous polypropylene.

These patterns display the five main diffractions characteristic of the α iPP modification [11]. Three different polymorphic modifications, α, β and γ, all sharing a three-fold conformation, have

been reported in iPP. In addition, a fast quenching of iPP leads to a phase of intermediate or mesomorphic order [12]. Estimation of the amorphous component content at room temperature, obtained from the totally amorphous profile of an elastomeric PP sample, allows determination of the crystallinity degree from WAXS experiments by simple subtraction. The obtained values are very similar (0.65-0.70), independently of TiO_2 incorporation. However, effect of TiO_2 composition is mainly seen in relative variations of the intensity exhibited by several diffractions (0 4 0), (1 1 1) and (1 3 1, 0 4 1) as deduced from Fig. 1.

The WAXS/SAXS structural characterization indicates the relatively limited structural modification of the iPP matrix by effect of the anatase component presence. The single noticeable effect is the growth of the most probable crystal size, particularly in the Ti5 film. The essential constancy of the iPP structural characteristics is also evidenced with Raman, which, on the other hand provides also information about the inorganic component state of the nanocomposites. As judged by the invariant characteristics of the stronger E_g anatase peak at ca. 150 cm^{-1}, the TiO_2 component morphological characteristics seem to smoothly vary within the Tix series. SEM photographs demonstrated no microsized aggregated nuclei, indicating that TiO_2 nanoparticles have been highly dispersed within the iPP matrix and their practical absence at the surface of the material. This contrast with the microsized aggregates typically observed in other polyolefin-based nanocomposites with similar incorporations to the ones used in this study [13]. The absence of the oxide at the surface of the materials was further confirmed using the sensitive EPR technique with the assist of O_2 as a probe molecule. The noticeable homogeneity of the Tix materials at the nanometer scale indicated by the SEM study is only possible because of the use of a coupling agent as well as the correct surface/size characteristics of the nano-oxide. To confirm this aspect, a TEM study of the Ti2 sample bulk was performed. In this case, the oxide is dispersed in the polymeric matrix exhibiting nanometer-scale aggregates ranging from 10 (the oxide primary particle size) to 200 nm, with an average size (Feret diameter) of 80 nm (± 20 nm). Considering that the titania preparation makes use of an oxide previously calcined at high temperature (500 ^oC) to ensure the exclusive presence of the anatase polymorph (e.g. absence of an amorphous contribution) and the strict control of its biocidal capabilities, the nanometric dispersion of the oxide reached for loadings below 5 wt% is significant, particularly with respect to micro-sized or bulk titania specimens [6], or comparing with other inorganic components (clay, SiO_2) introduced in polyolefins using a similar procedure (e.g. melting process) [13].

The combined UV excitation (UV-vis spectroscopy) and de-excitation (photoluminescence spectroscopy)/EPR analysis confirms that upon light excitation the organic/polymeric component located at the surface of the material handles holes primarily originated at the oxide. The exact transfer mechanism from oxide holes to polymer is unknown; however, as the thermodynamic driving force of this phenomenon depends on both organic and inorganic conduction band edges, the managing of these two energy levels may increase the effectiveness of the transfer process. As a final effect, such charge carriers would be efficiently involved in the photo-killing of microorganisms for samples having TiO_2 content above 1 wt. %.

Antimicrobial properties of the resulting nanocomposites films were tested against Gram negative *P. aeruginosa* and Gram positive *E. faecalis* (Fig 2). We remark that both are antibiotic-resistance and clinically isolated strains, magnifying the interest of the present study. Some differences are visible in the performance of the different Tix nanocomposite films with respect to the two microorganisms tested. A significant effect is already observed with the Ti0.5 samples in the case of *P. aeruginosa* while the influence of the oxide on the biocidal activity is more gradual for *E. faecalis*. Common to both experiments is that maximum performance is obtained using the Ti2 film. For that sample, almost complete cell inactivation of both microorganisms is reached, accounting for a log-reduction of near ca. 8 units.

Comparison with other biocidal agents allows concluding that our systems display an unprecedented power for bacteria destruction. Concerning *P. aeruginosa,* our maximum ca. 8-9 log-reduction in 0.5 h can be compared with those observed using TiO_2 either as a powder (Degussa P25; 3.5 log-reduction/0.67 h) [14] or supported on Plexiglas (5.4 log-reduction/1 h) [15] and

ethylene-vinyl alcohol copolymer (EVOH; 8.3 log-reduction/0.5 h) [16]. Comparison with reported results using Ag-based systems as commercial AgION coating stain steel (1.6 log-reduction/4 h) [17] or simple chemicals like glutaraldehyde, formaldehyde, H_2O_2, phenol, cupric ascorbate or sodium hypochlorite (all below 6 log-reduction/0.5 h) [18] highlights the potential of our systems. The performance with *E. faecalis* is less studied but as a Gram positive bacterium has a thicker and more compact cell wall than the other microorganism of our study and thus is potentially more difficult to eliminate. Our result (ca. 8-9 log-reduction/0.5 h) can be compared with water suspension of TiO_2 promoted with Pt (IV) salts (ca. 6 log-reduction/0.5 h) [19] or TiO_2 –Ni contains (2 log-reduction for extended period of times) [20]. Other biocides based on simple chemicals as trichlorosan on styrene-acetate copolymers (initial rate enhancement below 2 with respect to the polymer alone) [21]; organometallic complexes leading to oxygen radical formation (3.5 log-reduction/4 h) [22]; or UV-treated Nylon (1.8 log-reduction/6 h) [23] provide further support to our conclusion concerning the good performance of these nanocomposite films here described. The combined analysis of both microorganisms is thus illustrative of the biocidal potential of these films which showed a satisfactory performance if compared with most of the biocidal agents reported up date. These systems may find use for a wide variety of food packaging, biomedical, coating for "clean" solid surfaces or general disinfection applications.

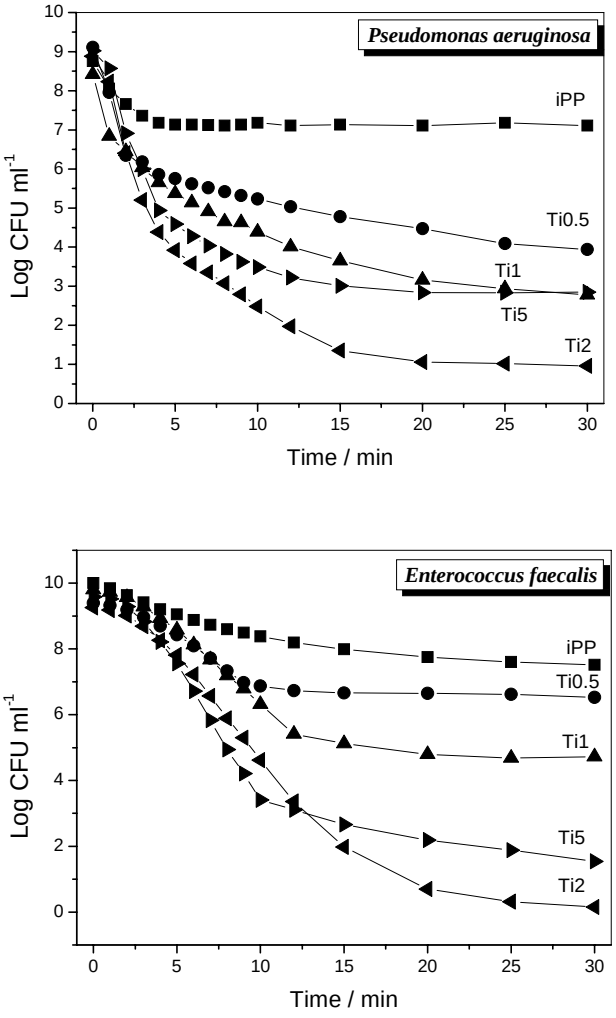

Figure 2. Process come-up logarithmic reduction of microorganism population suspended in Luria-Bertani medium. Survival curves of *P. Aeruginosa* and *E. faecalis* as a function of the irradiation time for Tix and iPP control samples.

ACKNOWLEDGEMENTS
Financial support from CSIC and MEC is acknowledged by Dr. A. Kubacka and Ms. C. Serrano for their I3P postdoctoral and FPU predoctoral grants, respectively. This work was supported by the CSIC under the projects PIF20058F0101, PIF200560F0102, PIF200560F103 and PIF200570F104. The synchrotron work was supported by the European Community-Research Infrastructure Action under the FP6 "Structuring the European Research Area" Programme (through the Integrated Infrastructure Initiative "Integrating Activity on Synchrotron and Free Electron Laser Science"), contract RII3-CT-2004-506008 (IA-SFS).

REFERENCES

1. Carp O., Huisan C.L., Reller A., Prog. Solid State Chem. (2004) 32 33-117.
2. (a) Galli P., Vecellio G., Prog. Polym. Sci. (2001) 26 1287-1336.
(b) Galli P., Vecellio G., J. Polym. Sci. Polym. Chem. Ed. (2004) 42 396-415.
3. Resconi L., Cavallo A., Fait F., Chem. Rev. (2000) 100 1253-1346.
4. Appendini P., Hotchkiss J.H., Innovative Food Sci. Emerg. (2002) 3 113-126.
5. Fernández-Garcia M., Wang X., Belver C., Hanson, J.C., Rodriguez J.A., J. Am. Chem. Soc. (2007) 129 13604-13612.
6. (a) Fan X.S., J. Vinyl Add. Technol. (2007) 13 65-70.
(b) Supaphol P., Thanomkiat P., Jonkesen J., Dangtungee R., Polym. Test. (2007) 26 20-37.
(c) García-Lopez D., Picazo O., MarinoJ.C., Pastor J.M., Eur. Polym. J. (2003) 39 945-950.
7. Bikiaris D.N., Vassilou A., Pavlidou E., Karayannidis G.P., Eur. Polym. J. (2005) 41 1965-1978.
8. Mansel S., Pérez E., Benavente R., Pereña J.M., Bello A., Röll W., Kirsten R., Beck S., Brintzinger H.H., Macromol Chem. Phys. (1999) 200 1292-1297.
9. Ferrer M., Soliveri J., Plou F.J., López-Cortés N., Reyes-Duarte D., Christensen M., Copa-Patiño J.L., Ballesteros A., (2005) 36 391-398.
10. Cerrada M.L., Serrano C., Sánchez-Chaves M., Fernández-García M., De Andrés A., Riobóo R.J., Fernández-Martín F., Kubacka A., Ferrer M., Fernández-García M., Environ. Sci. Technol. (2009) 43 1630-1634.
11. Turner-Jones A., Aizlewood J.M., Becket D.R., Makromol. Chem. (1964) 75 134-158.
12. Arranz-Andrés J., Benavente R., Pérez E., Cerrada M.L., Polym.J. (2003) 35 766-777.
13. Ma D., Akpalu Y.A., Li Y., Siegel R.W., Schadler L.S., J. Polym. Sci. Part B: Polym. Phys. (2005) 43 488-497.
14. Ibañez J.A., Litter M.I., Pizarro R.A., J. Photochem. Photobiol. A (2003) 157 81-85.
15. Kuhn K.P., Chaberny I.F., Massholder K., Sticker M., Benz V.W., Sonnatg H.G. Erdiner L., Chemosphere (2003) 53 71-77.
16. Kubacka A., Serrano C., Ferrer M., Lundsford H., Bieleck P., Cerrada M.L., Fernández-García M., Fernández-García M., Nano Lett. (2007) 7 2529-2534.
17. Cowan M.M., Abshire K.Z., Houk S.L., Evans S.M. J.Ind. Microbiol. Biotechnol. (2003) 30 102-106.
18. Sagripanti J.C., Bonifacio A., J. AOAC Int. (2000) 83 1415-1422.
19. Mitoraj D., Jancyk A., Strus M., Stochel G., Heczko P.B., Macyk W., Photochem. Phothobiol. Sci. (2007) 6 642-648.
20. Zhi-hong Z., Sakagami Y., Osaka T., Chem. Lett. (1997) 26 909-911.
21. Chung D., Papadakis S.E., Yam K.L., J. Food Sci. Technol. (2003) 38 165-169.
22. Villén L., Majón F., García-Resnadillo D., Orellana G., Appl. Catal. (2006) B 69 1-9.
23. Shearer A.E.H., Park J.S., Hoover D.G., Hayne S.L., Biotechnol. Bioeng. (2000) 67 141-146.